1828
AKADÉMIAI KIADÓ

Zirconia-alumina ceramics: A study of their properties

Rusul Ahmed Shakir* and Róbert Géber

Faculty of Materials and Chemical Engineering, Institute of Energy – Ceramic and Polymer Technology, University of Miskolc, Miskolc-Egyetemváros, Hungary

Pollack Periodica • An International Journal for Engineering and Information Sciences

20 (2025) 3, 39–44

DOI: 10.1556/606.2025.01253
© 2025 The Author(s)

Received: November 19, 2024 • Revised manuscript received: January 5, 2025 • Accepted: January 14, 2025
Published online: May 22, 2025

ORIGINAL RESEARCH PAPER

ABSTRACT

The current investigation shed light on examining the properties of ceramic based composites manufactured with various percentages of alumina and zirconia. Compressive strength, volumetric shrinkage, apparent porosity, and apparent density of the ceramic composites were the most significant outputs that impacts the composites quality. Therefore, this paper aims to evaluate the resulted composites according to these outputs' response. It was noted that the dominant peaks in the X-ray diffraction results is tetragonal zirconia in spite of using monoclinic zirconia during the composites manufacturing. The optimum compressive strength of 370 MPa was emerged with specimens after sintering produced with 70 wt.% zirconia and 30 wt.% alumina. Moreover, the zirconia-alumina composites findings revealed a remarkable improvement when compared with ceramics made from these materials individually.

KEYWORDS

alumina, monoclinic-zirconia, tetragonal-zirconia, magnetic stirrer, compressive strength

1. INTRODUCTION

Ceramics have been the subject of intense study in materials science and engineering due to the growing need for these materials with improved characteristics for a wide range of application [1, 2]. Zirconia (ZrO_2) and alumina (Al_2O_3) ceramics have become popular materials for various applications due to their unique properties when compared with other ceramics [3]. The addition of zirconia in the fabricated zirconia-alumina composites improves fracture toughness, whilst alumina contributes to increased compressive strength. Zirconia and alumina ceramics, when combined, could improve each material's characteristics, leading to higher-quality composites [4–8]. Nonetheless, challenges related to processing and material homogeneity emerge when attempting to attain a dense and uniform distribution of these components in a compressed form. The mixing of various material powders was mostly accomplished via ball milling [9–15] and magnetic stirrers [16–20]. Magnetic stirring can occasionally be a simpler and quicker option since it does not need as complicated of equipment. There are fewer moving components and less labor-intensive procedures involved in its setup, cleaning, and maintenance compared to ball milling. Generally, magnetic stirring is more energy-efficient than ball milling. The ball mill necessitates more energy for moving the substantial grinding balls. Ultimately, using a magnetic stirrer for mixing ceramic powder results in reduced operational costs and mitigates environmental harm. The magnetic stirrer ensures that the powder particles remain intact and unchanged in form throughout the mixing process, protecting the ceramic material's characteristics. Unlike ball milling, which may introduce impurities from metal or abrasive wear into the ceramic powder via the grinding media, magnetic stirring mitigates this risk by limiting direct contact between the stirring elements and the powder. This is of the highest significance, particularly when dealing with high-purity or specialist ceramics, because characteristics may be affected by even minute quantities of impurities [21, 22].

*Corresponding author.
E-mail: rusulahmed1990@gmail.com

Brought to you by MTA Könyvtár és Információs Központ olvasók | Unauthenticated | Downloaded 11/03/25 08:29 AM UTC

This study used inexpensive and easy procedures to fabricate a zirconia-alumina ceramic structure with enhanced characteristics. The process begins with mixing zirconia and alumina powders with distilled water and deflocculant. The mixture is then cast into a sheet, dried, and finally crushed into fine particles. Following this, a universal compacting apparatus was used to compress the fine ceramic particles. Analysis of the prepared samples is carried out to determine their compressive strength, microstructure, volume shrinkage, apparent porosity, and apparent density. This study aims to explore the effectiveness of utilizing stirring and compacting methods in the production of high-density zirconia-alumina ceramic composites.

2. MATERIALS AND EXPERIMENTAL METHODS

Magnetic stirring and compacting techniques were used to produce densely structured ceramic composites containing varying concentrations of zirconia and alumina. The zirconium oxide powder (ZrO_2) used in this research was monoclinic zirconia from Interkeram Ltd., a distributor. It has a density of around 5.71 g cm^{-3} and a purity level of 99.99 wt.%. Zirconia particles had an average size of 0.1 µm, as it is shown by the Scanning Eelectron Mmicroscopy (SEM) analysis. Alumina (Al_2O_3), from Interkeram Ltd., a distributor, was used as an additional oxide to improve the characteristics of zirconia. The purity of alumina is around 99.99 wt.%, whereas its density that determined using a pycnometer, yielding about 3.04 g cm^{-3}. The average size of alumina particles was around 0.29 µm. Dolapix CE64 (prepared by Zschimmers and Schwartz in Germany) was used as a deflocculant to disperse ceramic particles in the solution and to inhibit their agglomeration. To prepare dense-structured composites, various concentrations of raw ceramic powders were combined using a magnetic stirrer along with a suitable quantity of deflocculant and distilled water. The numerous structure mixed compositions used for this investigation are listed in Table 1. Suspension concentration expresses the solid to liquid ratio.

The suspensions were stirring for two hours at room temperature with 600 rpm as the stirring speed. The produced slurries were placed onto the plastic sheet and left to dry at room temperature for duration of two days. Upon completion of the drying process, a thin layer of well-blended ceramic powders is produced, which may be readily crushed and refined to acquire particles that can be compressed. The ceramic powder mixtures that had been produced were compressed into a cylindrical form using a universal compacting machine, with a diameter of about 8.5 mm and a height of about 17 mm. The specimens were fabricated via a heat-treated metal mold, applying a compressive force of roughly 100 MPa (equivalent to 5600 N), and a displacement speed of 2 mm min^{-1}. Figure 1 shows some of the prepared compacting ceramic composites.

Table 1. Mix compositions for dense-structured samples (in wt.%)

m-ZrO_2	Al_2O_3	Deflocculant	Suspension Conc.
85.0	15.0	1.5	60
82.5	17.5	1.5	60
80.0	20.0	1.5	60
77.5	22.5	1.5	60
75.0	25.0	1.5	60
72.5	27.5	1.5	60
70.0	30.0	1.5	60

3. PRE-SINTERING AND SINTERING PROCEDURE

The laboratory furnace was set to 500 and 1,100 °C to pre-sinter the ceramic samples. Every temperature was held for two hours with the samples. The pre-sintering technique included heating the samples to 1,100 °C at a rate of 2 °C min^{-1}. Following the pre-sintering process, the samples were subjected to a continuous cooling cycle in the furnace until they reached room temperature. Figure 2 displays the dense specimens' pre-sintering profile.

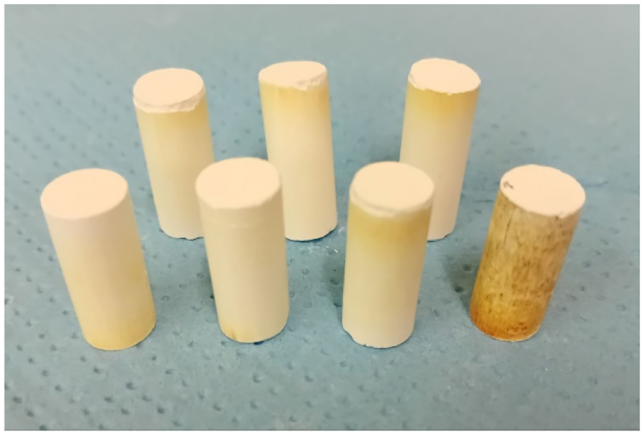

Fig. 1. The prepared compacted ceramics

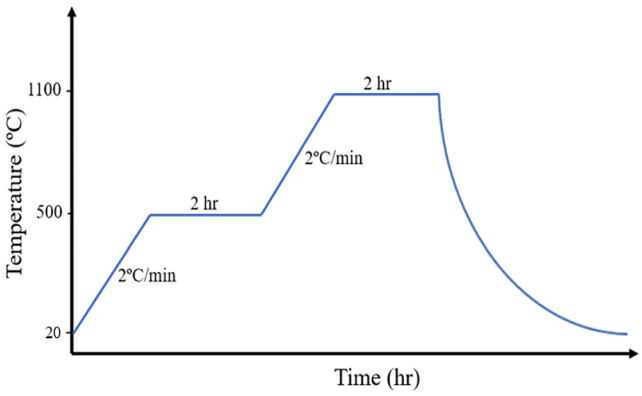

Fig. 2. The pre-sintering profile

Brought to you by MTA Könyvtár és Információs Központ olvasók | Unauthenticated | Downloaded 11/03/25 08:29 AM UTC

After the ceramic samples were pre-sintered, they were subjected to a slow sintering procedure in the lab furnace. The sintering procedure was carried out at heating rates of 2 °C min^{-1} and temperatures of 300, 500, and 1,600 °C. First, the samples were heated to 300 °C and 500 °C for one hour each. Then, they were heated to 1,600 °C for two hours. After the sintering process had been completed, the specimens were left in the furnace to cool down to room temperature. Dense structured specimens' sintering profile is shown in Fig. 3.

4. CHARACTERIZATION METHODS

The particles' morphology of zirconia and alumina ceramic was evaluated using SEM. Due to the non-conductive nature of ceramic, a conductive gold coating must be added to the ceramic powder to mitigate charging effects. Prior to entering the SEM chamber, the ceramic powders were meticulously affixed to adhesive tape and then covered with a coating of gold. The phase composition of the synthesized ceramics was determined by means of an X-Ray Diffraction (XRD) analysis with Cu Kα radiation in the 2Θ range of 3–90°. The step width was 0.01, and the exposure duration each place was 2 s. Utilizing the universal testing equipment, the compressive strength of the produced ceramics was evaluated. The sintered samples used for this evaluation measure 17 mm in length and 8 mm in diameter. Under room temperature conditions, the loading rate used in this experiment was 2 mm min^{-1}. Using a micrometer caliper and weighing equipment, the length and weight of both pre-sintered and sintered samples were measured. In order to determine the samples' apparent densities, these measurements were conducted three times. A ceramic composite sample's apparent porosity was determined using the water absorption technique. Following this, the volume of the samples was measured before pre-sintering and sintering (V_0) and the volume of the samples after pre-sintering and sintering (V_1) and used the following equation to determine the volume shrinkage of each sample after pre-sintering and sintering. The samples' volumes (VS) are determined by averaging three readings from a digital Vernier caliper,

$$VS = \frac{V_0 - V_1}{V_0} \cdot 100\%. \quad (1)$$

5. RESULTS AND DISCUSSION

SEM was used to analyze the particle morphology of the ceramics. As can be seen in the scanning electron micrograph presented in Fig. 4a, pure zirconia powder was found to be a combination of spheroidal, narrow-sized particles with a range diameter of approximately 0.1 µm. Figure 4b illustrates that the particles of pure alumina powder exhibit approximately longitudinal forms with a diameter range of around 0.29 µm.

Density and porosity are critical characteristics influencing mechanical characteristics. Composites exhibiting increased density and reduced porosity provide superior mechanical characteristics [23]. Porosity may diminish the resistance to fractures by decreasing the resistive surface due to stress concentration effects in the pores. The reduction of the porosity and the development of composites with increased density are crucial for achieving superior mechanical characteristics. Possible densification enhancements could result from a more uniform distribution of the mixture's phases, like lumina and zirconia. As a result of thermal assistance, powdered particles densified during the sintering process. Thermal energy accelerates the diffusion of atoms, hence establishing bonding between neighboring particles. The ongoing provision of heat energy increases the number of contact sites among particles, while the intervening porosity disperses from the contact zone. Consequently, a significant rise in density occurred, leading to a reduction in the porosity of the composite. Additionally, the present grains inside the particle might increase to reduce the systems' total energy. Consequently, densification and grain growth transpire concurrently. Figure 5 illustrates the correlation between apparent densities and alumina content following the pre-sintering and sintering of ceramic composites.

Results show that both the pre-sintered and sintered samples' apparent densities are inversely correlated with their alumina concentration. The apparent density of the

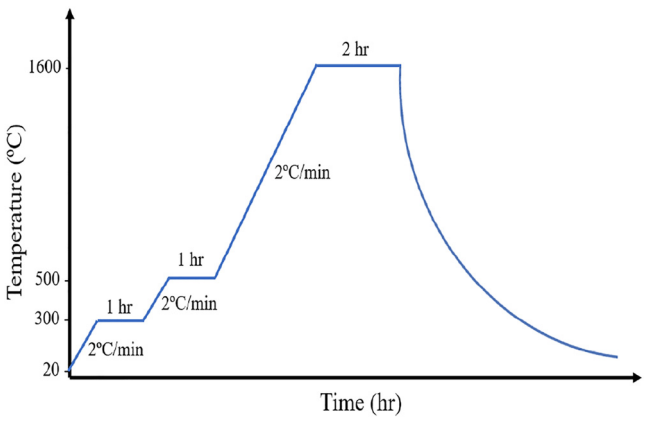

Fig. 3. The sintering profile

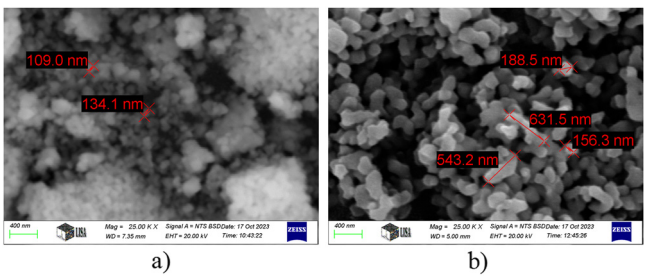

Fig. 4. SEM micrograph of a) zirconia powder, b) alumina powder

Brought to you by MTA Könyvtár és Információs Központ olvasók | Unauthenticated | Downloaded 11/03/25 08:29 AM UTC

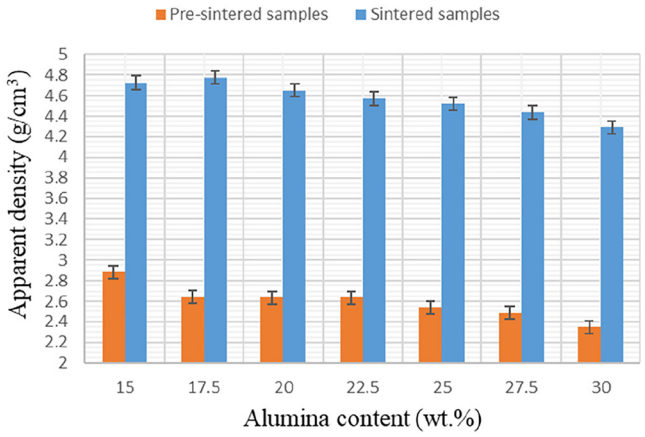

Fig. 5. Apparent density via Al_2O_3 content for compacted ceramics

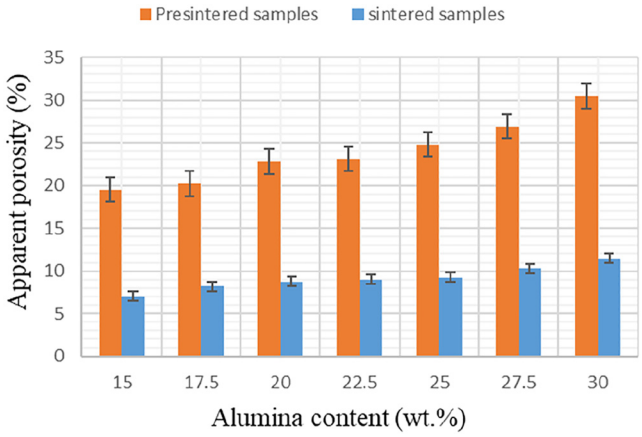

Fig. 6. Apparent porosity via Al_2O_3 content for compacted ceramics

samples diminishes as the alumina percentage increases. Alumina has a lower density than zirconia, at about 3.04 g cm^{-3}, hence as the alumina concentration increased, the density decreased. Zirconia's density is around 5.71 g cm^{-3}. Pre-sintering and sintering heating at a low rate of 2 °C min^{-1} allowed for excellent particle diffusion and binding, leading to pore minimization. The calculated apparent density of pre-sintered compacted samples ranges from approximately 2.88 g cm^{-3} for a sample prepared with 15 wt.% alumina to about 2.34 g cm^{-3} for a sample prepared with 30 wt.% alumina. While the calculated apparent density of sintered compacted samples ranges from approximately 4.72 g cm^{-3} for a sample prepared with 15 wt.% alumina to about 4.47 g cm^{-3} for a sample prepared with 30 wt.% alumina. The findings indicated that the tiny pores of uniform dimensions underwent higher densification in the fine-particles matrix with a greater concentration of zirconia, compared to the coarse-particles matrix with a higher content of alumina. These findings suggest that the process of densification was influenced by both thermodynamic and kinetic factors. The kinetic factors were more favorable in the fine-particles zirconia-rich matrix compared to the coarse-particles matrix containing higher concentration of alumina. The density of the ceramic composite samples is directly proportional to its porosity; few pores in a structure can result in approximately complete densification. The increased porosity of the produced samples is causing a reduction in their density. As it is shown in Fig. 6, the produced ceramic composites' apparent porosity test results are shown after pre-sintering and sintering.

Figure 6 shows that alumina has significant impacts on the sample porosities, which in turn affects the densities of ceramics. When alumina was added to all the samples, the apparent porosity increased. Pre-sintered samples with 15 wt.% alumina have an estimated computed apparent porosity of around 19%, whereas samples with 30 wt.% alumina have an apparent porosity of about 30%. While sintered samples made with 15 wt.% alumina has an apparent porosity of about 7% and samples prepared with 30 wt.% alumina have an apparent porosity of around 11%. Figure 7 shows that the volume shrinkage, in relation to sample density, decreases as the fraction of ceramic alumina powder in the solution rises. Figure 7 shows that compacted samples after pre-sintering have values of volume shrinkage, ranging from 8% for the sample made with 15 wt.% alumina to 5% for the sample made with 30 wt.% alumina. While the volume shrinkage of the sintered samples was ranges from 20% for the sample contain 15 wt.% alumina to 11% for the sample contain 30 wt.% alumina. With a rise in alumina concentration, the total volume shrinkage of the composite may diminish. This is owing to alumina's reduced susceptibility to shrinkage compared to zirconia during sintering, attributable to its elevated melting point and diminished the ability to sintering. Higher alumina concentration may serve as a barrier to shrinkage, diminishing the overall volume contraction.

Figure 8 illustrates the XRD pattern of a sintered zirconia-alumina composite, comprising 70 wt.% monoclinic zirconia and 30 wt.% alumina, which confirming the creation of a multi-phase composite.

After sintering process, three phases namely monoclinic zirconia (m-ZrO_2), tetragonal zirconia (t-ZrO_2), and corundum alumina (α-Al_2O_3) were produced. There were

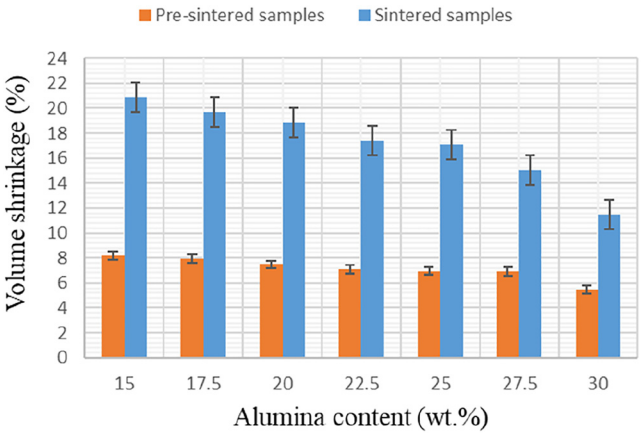

Fig. 7. Volume shrinkage via Al_2O_3 content for compacted ceramics

Brought to you by MTA Könyvtár és Információs Központ olvasók | Unauthenticated | Downloaded 11/03/25 08:29 AM UTC

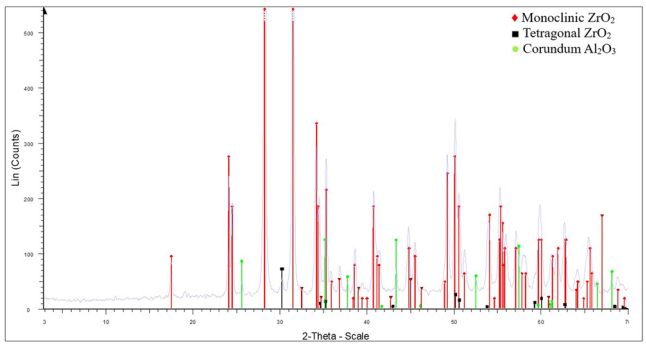

Fig. 8. XRD pattern of sintered zirconia-alumina composite

noticeable peaks of t-ZrO_2 even though m-ZrO_2 was employed to produce the composite. Figure 9 shows the compressive strength of dense-structured ceramics following the pre-sintering and sintering processes, with different concentrations of alumina.

The compressive strength increases, from ~100 to 127 MPa for pre-sintered samples and from ~279 to 370 MPa for sintered samples, with the increase in alumina content from 15 to 30 wt.%. The strength was significantly very high owing to the considerable high density and low porosity.

The enhancement in the strength of the zirconia-alumina composite is due to the shear strain and volume expansion caused by the transformation of ZrO_2 from tetragonal to monoclinic. In the situation that a stress fracture attempts to develop, each tetragonal particle releases energy and expands to a stable size in monoclinic form. A combination of t-ZrO_2 and m-ZrO_2 makes the composite stronger and more resistant to wear and tear. The hardness of the composite is affected by several factors, including Al_2O_3 and ZrO_2 particle sizes, the volume percentage of ZrO_2 kept in the metastable tetragonal phase, and the relative distribution of the two oxides in the matrix [24]. Decreasing the particle size of Al_2O_3 and ZrO_2 would enhance their uniform distribution and increase the likelihood of ZrO_2 being retained in a metastable tetragonal phase [25].

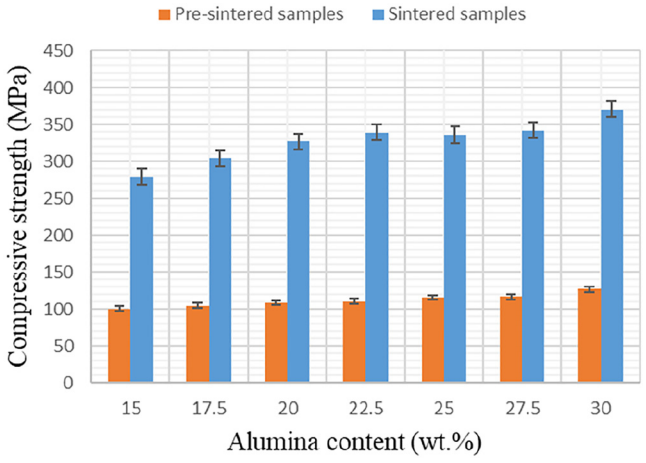

Fig. 9. Compressive strength via alumina content wt.%

6. CONCLUSION

The primary objective in this research was to determine how different amounts of alumina affected zirconia ceramics made utilizing a simple and inexpensive method of preparation. The X-ray diffraction evidence reveals the presence of tetragonal zirconia peaks, even though the composite was made from monoclinic zirconia and alumina. This signifies that alumina functions as a stabilizer for the tetragonal phase of zirconia. Because zirconia is denser than alumina, the apparent density test results indicate that the samples seem to have less density as the alumina content rises. As a result of the alumina content lowering the density, the findings of the apparent porosity test indicate that the amount of alumina has a positive correlation with the apparent porosity. The volume shrinkage test results show that the volume shrinkage, in relation to sample density, decreases as the alumina content increased. The compressive strength rises with the increase of alumina concentration, attributed to the shear strain and volumetric expansion resulting from the change of ZrO_2 from tetragonal to monoclinic.

ACKNOWLEDGMENTS

The Authors would like to express their gratitude to the University of Miskolc, particularly Institute of Energy – Ceramic and Polymer Technology to use their laboratories. This paper is supported by Hungary's TEMPUS Public Foundation and Stipendium Hungaricum Scholarship.

REFERENCES

[1] J. E. F. M. Ibrahim, E. Kurovics, M. Tihtih, and L. A. Gomze, "Ceramic bricks with enhanced thermal insulation produced from natural zeolite," *Pollack Period.*, vol. 16, no. 3, pp. 101–107, 2021.

[2] M. Osfouri and A. Simon, "Study on the thermal conductivity and density of foam glass," *Pollack Period.*, vol. 18, no. 1, pp. 126–131, 2023.

[3] R. A. Shakir and R. Géber, "Porosity and pore morphology characteristics of zirconia-alumina bioceramics," *Pollack Period.*, vol. 19, no. 3, pp. 107–114, 2024.

[4] S. R. Choi and N. P. Bansal, "Mechanical behavior of zirconia/alumina composites," *Ceramics Int.*, vol. 31, no. 1, pp. 39–46, 2005.

[5] M. Guazzato, M. Albakry, M. V. Swain, and J. Ironside, "Mechanical properties of in-ceram alumina and in-ceram zirconia," *Int. J. Prosthodont.*, vol. 15, no. 4, pp. 339–346, 2002.

[6] A. Karthik, S. R. Srither, N. R. Dhineshbabu, N. Lenin, S. Arunmetha, P. Manivasakan, and V. Rajendran, "Stabilization of tetragonal zirconia in alumina-zirconia and alumina-yttria stabilized zirconia nanocomposites: A comparative structural analysis," *Mater. Characterization*, vol. 158, 2019, Art no. 109964.

Brought to you by MTA Könyvtár és Információs Központ olvasók | Unauthenticated | Downloaded 11/03/25 08:29 AM UTC

[7] M. M. S. Wahsh, R. M. Khattab, and M. Awaad, "Thermo-mechanical properties of mullite/zirconia reinforced alumina ceramic composites," *Mater. Des.*, vol. 41, pp. 31–36, 2012.

[8] S. Sequeira, M. H. Fernandes, N. Neves, and M. M. Almeida, "Development and characterization of zirconia-alumina composites for orthopedic implants," *Ceramics Int.*, vol. 43, no. 1, Part A, pp. 693–703, 2017.

[9] W. Guo, Q. He, A. Wang, T. Tian, C. Liu, L. Hu, H. Wang, W. Wang, and Z. Fu, "Effects of ball milling on the densification behavior, microstructure, and mechanical properties of TiB_2-SiC ceramics," *J. Mater. Res. Technol.*, vol. 15, pp. 6700–6712, 2021.

[10] Q. Guo, S. Luo, J. Gan, J. Li, and L. Zhang, "Effect of ball milled Zr/Al/ZrB_2 composite powders on microstructure and toughening of ZrB_2–SiC/Zr–Al–C composite ceramics sintered by spark plasma sintering," *Mater. Sci. Eng. A*, vol. 644, pp. 96–104, 2015.

[11] L. B. Kong, T. S. Zhang, Y. Z. Chen, J. Ma, F. Boey, and H. Huang, "Microstructural composite mullite derived from oxides via a high-energy ball milling process," *Ceramics Int.*, vol. 30, no. 7, pp. 1313–1317, 2004.

[12] X. Zhang, Z. Zhang, B. Nie, H. Chen, Y. Wang, L. Zheng, Y. Bai, and W. Wang, "Microstructure and mechanical properties of fine-grained boron carbide ceramics fabricated by high-pressure hot pressing combined with high-energy ball milling," *Ceramics Int.*, vol. 44, no. 9, pp. 10766–10772, 2018.

[13] X. Xu, T. Nishimura, N. Hirosaki, R. Xie, and H. Tanaka, "Fabrication of a nano-Si_3N_4/Nano-C composite by high-energy ball milling and spark plasma sintering," *J. Am. Ceram. Soc.*, vol. 90, no. 4, pp. 1058–1062, 2007.

[14] M. Sorescu and T. Xu, "The effect of ball-milling on the thermal behavior of anatase-doped hematite ceramic system," *J. Therm. Anal. Calorim.*, vol. 103, pp. 479–484, 2011.

[15] E. Filipek and K. Wieczorek-Ciurowa, "Comparison between the synthesis in molybdenum and antimony oxides system by high-temperature treatment and high-energy ball milling," *J. Therm. Anal. Calorim.*, vol. 97, 2009, Art no. 105.

[16] A. A. Ariff, A. Supee, and M. Z. M. Yusop, "Influence of magnetic stirrer speed on the properties of chemical bath deposited FeS_xO_y thin films," *Materialstoday: Proc.*, vol. 110, pp. 38–44, 2024.

[17] R. Tahmasebi-Boldaji, S. Ghazanfari, H. R. Kuyakhi, N. T. Boldaji, and M. Torki, "Experimental investigation of ultrasonic cycle/magnetic stirrer (UC/MS) effect on water/α Al_2O_3 nanofluid stability and thermal conductivity and its ANFIS/PSO modeling," *Results Eng.*, vol. 19, 2023, Art no. 101284.

[18] S. Bicakci, H. Citak, H. Gunes, M. Coramik, and Y. Ege, "A new RMF stirrer design to reduce mixing time," *Eng. Sci. Technol. Int. J.*, vol. 58, 2024, Art no. 101850.

[19] M. M. Ballari, M. F. Edelmannová, R. Ricka, M. Reli, and K. Kočí, "Exploring kinetics and mass transfer in photocatalytic CO_2 reduction: Impact of photocatalyst loading and stirrer speed," *Energy Convers. Manag. X*, vol. 23, 2024, Art no. 100651.

[20] X. Fang and H. Zou, "Revisiting the preparation of cylindrical polystyrene particles by magnetic stirring," *Colloids Surf. A: Physicochemical Eng. Aspects*, vol. 638, 2022, Art no. 128308.

[21] W. D. Kingery, H. K. Bowen, and D. R. Uhlmann, *Introduction to Ceramics*, 2nd ed. John Wiley & Sons, 1976.

[22] M. N. Rahaman, *Ceramic Processing and Sintering*, 2nd ed. CRC Press, 2003.

[23] M. C. C. de D. B. Moraes, C. N. Elias, J. D. Filho, and L. G. de Oliva, "Mechanical properties of alumina-zirconia composites for ceramic abutments," *Mater. Res.*, vol. 7, no. 4, pp. 643–649, 2004.

[24] A. Bleier, P. F. Becher, K. B. Alexander, and C. G. Westmoreland, "Effect of aqueous processing conditions on the microstructure and transformation behavior in Al_2O_3-ZrO_2 (CeO_2) composites," *J. Am. Ceram. Soc.*, vol. 75, no. 10, pp. 2649–2658, 1992.

[25] R. C. Garive, "Occurrence of meta-stable tetragonal zirconia as a crystallite size effect," *J. Phys. Chem.*, vol. 69, no. 4, pp. 1238–1243, 1965.

Open Access statement. This is an open-access article distributed under the terms of the Creative Commons Attribution 4.0 International License (https://creativecommons.org/licenses/by/4.0/), which permits unrestricted use, distribution, and reproduction in any medium, provided the original author and source are credited, a link to the CC License is provided, and changes – if any – are indicated. (SID_1)

Brought to you by MTA Könyvtár és Információs Központ olvasók | Unauthenticated | Downloaded 11/03/25 08:29 AM UTC